



Swansea University  
Prifysgol Abertawe



## Cronfa - Swansea University Open Access Repository

---

This is an author produced version of a paper published in:  
*Journal of Plankton Research*

Cronfa URL for this paper:  
<http://cronfa.swan.ac.uk/Record/cronfa40800>

---

### Paper:

Munk, P., Nielsen, T., Jaspers, C., Ayala, D., Tang, K., Lombard, F. & Riemann, L. (2018). Vertical structure of plankton communities in areas of European eel larvae distribution in the Sargasso Sea. *Journal of Plankton Research*  
<http://dx.doi.org/10.1093/plankt/fby025>

---

This item is brought to you by Swansea University. Any person downloading material is agreeing to abide by the terms of the repository licence. Copies of full text items may be used or reproduced in any format or medium, without prior permission for personal research or study, educational or non-commercial purposes only. The copyright for any work remains with the original author unless otherwise specified. The full-text must not be sold in any format or medium without the formal permission of the copyright holder.

Permission for multiple reproductions should be obtained from the original author.

Authors are personally responsible for adhering to copyright and publisher restrictions when uploading content to the repository.

<http://www.swansea.ac.uk/library/researchsupport/ris-support/>

1 Vertical structure of plankton communities in areas of  
2 European eel larvae distribution in the Sargasso Sea.

3

4 Peter Munk<sup>1\*</sup>, Torkel Gissel. Nielsen<sup>1</sup>, Cornelia Jaspers<sup>1,2</sup>, Daniel J. Ayala<sup>1</sup>, Kam W. Tang<sup>3</sup>, Fabien  
5 Lombard<sup>4</sup>, Lasse Riemann<sup>5</sup>.

6 1. National Institute of Aquatic Resources, Technical University of Denmark, 2800 Lyngby,  
7 Denmark

8 2. Helmholtz Centre for Ocean Science, GEOMAR, 24105 Kiel, Germany

9 3. Department of Biosciences, Swansea University, Swansea, SA2 8PP, United Kingdom

10 4. Sorbonne Université, CNRS-INSU, Laboratoire d'Océanographie de Villefranche, LOV UMR  
11 7093, F-06230 Villefranche-sur-mer, France

12 5 Marine Biology Section, Department of Biology, University of Copenhagen, 3000 Helsingør,  
13 Denmark

14

15 Keywords: vertical migration, plankton communities, leptocephali larvae, freshwater eels,  
16 Subtropical Convergence Zone

17

18 Running title: Vertical structure of plankton in the Sargasso Sea

19

20 \*Corresponding author: Peter Munk. E-mail address: pm@aqua.dtu.dk

21

## 22 **Abstract**

23 The European and American eels spawn in the Subtropical Convergence Zone (STCZ) in the  
24 Sargasso Sea, a dynamic and relatively productive area that is strongly influenced by front and eddy  
25 formations and subducted high-saline water masses. To understand how the physical and biological  
26 environments may affect the early life history of eels, we conducted a detailed bio-physical  
27 investigation of the water column at a site of high eel larvae abundance. Diel measurements and  
28 sampling in the upper 300 m revealed strong variations in hydrographic conditions and mean depths  
29 of different taxonomic groups; however, characteristic patterns of distribution were apparent. Most  
30 species showed diel vertical migrations, ascending about 20-30 m at night, whereas examples of  
31 nighttime downward migration were also seen. European eel larvae were among the species  
32 showing more extensive diel vertical migration: their population mean depth changed from 160 m at  
33 day to 100 m at night where abundance peaked at 45 m depth. Distribution and migration of eel  
34 larvae corresponded to patterns observed for small hydrozoans, supporting a proposed predator-prey  
35 linkage. The study demonstrates the diverse and vertically strongly structured plankton community  
36 of STCZ where larvae of eel and other fish find a wide range of potential niches.

37

38

## 39 **Introduction**

40 The Subtropical Convergence Zone (STCZ) in the Sargasso Sea is known to be a hotspot for  
41 spawning of Atlantic eels (Schmidt, 1923; Miller, 2014). Due to a sharp decline in recruitment to  
42 the eel populations in the recent decades, there is a strong demand for further understanding of the  
43 temporal and spatial variabilities in the bio-physical characteristics of the zone and how they may  
44 influence recruitment success. In the STCZ, warm tropical water meets colder North Atlantic water  
45 masses and the zone is bordered by hydrographic fronts of changing intensity and location (Eriksen  
46 *et al.*, 1991, Ullman *et al.*, 2007). Furthermore, the STCZ is characterized by significant eddy  
47 formation (Halliwell *et al.*, 1991) leading to intensive mixing in the upper 200-300 m (Munk *et al.*,  
48 2010; Richardson and Bendtsen, 2017). While the deep current (the North Equatorial Current) is  
49 directed towards the west, the upper layers in the zone might in some areas flow north-east along  
50 the zonal density fronts, forming an eastward Subtropical Counter Current (SCC) (Cushman-Roisin,  
51 1984). A thermocline is present at 100-150 m and an intrusion of more saline water originating  
52 from the equatorial areas is often seen at 80-150 m (Williams, 2001). The pronounced variability in  
53 the horizontal and vertical hydrography is likely to affect the structuring of plankton communities in  
54 the area with further influence on the early development of the anguillid eels (*Anguilla anguilla* and  
55 *A. rostrata*).

56 Studies of the plankton communities in the Sargasso Sea often target areas north of the STCZ, in  
57 particular the site of the Bermuda Atlantic Time-series Study (BATS) (reviewed by Steinberg *et al.*,  
58 2001). Conditions in these colder north-Atlantic waters are, however, not comparable to the STCZ,  
59 where the different hydrography would favor different plankton communities (Longhurst, 1985).  
60 Studies specifically targeting central areas of the STCZ have found an enhanced abundance of  
61 primary producers (Riemann *et al.*, 2011) and elevated productivity (Richardson and Bendtsen,  
62 2017). Although the Sargasso Sea is generally considered as oligotrophic with a predominance of  
63 picoplankton (Gasol *et al.*, 1997), the biomass of large protists, such as athecate dinoflagellates and  
64 ciliates, has been found to equal or exceed that of picoplankton within the STCZ (Riemann *et al.*,  
65 2011), probably leading to a locally enhanced mesozooplankton production. An enhancement in a  
66 number of metazoan groups, e.g. copepods and appendicularians, has been observed in central areas  
67 on STCZ (Munk *et al.*, 2010; Andersen *et al.*, 2011). Furthermore, fish larvae including those of  
68 European and American eels have been found in relatively high abundances within STCZ, with

69 declining abundances when passing the fronts towards waters outside the STCZ (Ayala *et al.*,  
70 2016).

71 In addition to horizontal variability in plankton community composition and abundances in the  
72 STCZ, variability is also apparent along the vertical axis, where most plankton taxa are  
73 concentrated in specific depth strata (Riemann *et al.*, 2011; Andersen *et al.* 2011). The published  
74 information on vertical distribution of fish larvae in the STCZ is restricted to distributional patterns  
75 of leptocephali larvae. In the western Sargasso, Miller (2015) found the majority of leptocephali  
76 larvae in the upper 100 m at night, with several species (including *Anguilla rostrata*) concentrated  
77 within the 50-60 m depth. Likewise, Castonguay and McCleave (1987) observed that at nighttime,  
78 *Anguilla* spp. larvae were concentrated within 50-70 m. *Anguilla* spp. larvae have been observed to  
79 perform marked diel vertical migrations, descending to 100-200 m depth during the day (Schoth  
80 and Tesch, 1982). However, only a few eel larvae have been found below a depth of 200 m  
81 (Schmidt, 1923; Castonguay and McCleave, 1987).

82 The early life of fishes in the STCZ, including the *Anguilla* spp., is governed by the specific  
83 physical, chemical and biological characteristics of available habitats in the water column. In order  
84 to gain further understanding of opportunities and constraints to the life of *Anguilla* spp. larvae, we  
85 here investigate in detail the water column properties and the structuring of the plankton community  
86 of the STCZ, looking for commonalities and differences between community members. We  
87 included several trophic levels, ranging from algae and microplankton, to mesozooplankton and  
88 macroplankton, and finally onto the fish larvae. The study was carried out during a larger field  
89 investigation at a site of relative high abundances of *Anguilla* spp, and we hypothesized that the eel  
90 larvae occupy a specific niche in the community, defined by their vertical position, their diel  
91 migration pattern and their linkages to specific hydrographical and biological characteristics.

92

## 93 **Materials and methods**

94 Intensive sampling was conducted at 25°38' N, 62°48'W from 31 March 13:46 UTM to 1 April  
95 14:20 UTM, 2014 on board of the R/V Dana (local time was UTM – 4 hours). The site was part of a  
96 survey transect across the STCZ, extending along 62°45'W from 24°40'N to 29°50'N (Fig. 1), and  
97 was chosen for the relatively high *A. anguilla* abundances observed during the standard transect  
98 sampling.

99 Profiles of temperature, salinity, fluorescence, oxygen and irradiance were measured from surface  
100 to 400 m depth by a Seabird SBE11 (9+) CTD, with mounted Biospherical QSP-2300L PAR  
101 Sensor, SBE 43 Dissolved Oxygen Sensor, and Turner Cyclops-7 Fluorometer. Silicate, nitrite,  
102 nitrate and chlorophyll *a* were measured in subsamples from ten-liter Niskin bottle samples taken at  
103 10, 30, 60, 85, 130, 155, 255 and 400 m depths.

104 An Underwater Video Profiler (UVP5, serial number Sn003, pixel size ca. 0.147; Picheral *et al.*,  
105 2010) was deployed alongside the CTD to 400 m. The device emitted flashes of red LED light that  
106 illuminated 0.93L of the water. Images of all particles within the illuminated area were recorded  
107 and analyzed for abundances in defined size ranges. Objects larger than 30 pixels were further  
108 analyzed by a taxonomist. Here we only report observations of particles in three size ranges: small  
109 (0.05-0.53 mm), medium (0.53-1.06 mm), and large (1.06-4.0 mm).

110 Microzooplankton (ciliates and heterotrophic dinoflagellates) were analyzed using water  
111 subsamples from ten-liter Niskin bottle samples taken at 10, 30, 60, 85, 130, 155, 255 and 400 m  
112 depths. These were immediately fixed with acid Lugol's solution (2% final concentration) and  
113 stored in the dark at 5°C until analysis. For the analysis, protozoans were allowed to settle for 24 h  
114 in 50-ml sedimentation chambers, and were then enumerated and sized under an inverted  
115 microscope (Utermöhl, 1958). Cells were identified to the lowest possible taxonomic level and  
116 grouped by equivalent spherical diameter intervals of 10 µm. Cell volumes were estimated from  
117 appropriate geometric formulae and converted to carbon content. All athecate dinoflagellates of  
118 unknown trophic type were considered heterotrophic (Andersen *et al.*, 2011).

119 Zooplankton samples were collected using a multiple opening-and-closing net (Multinet Midi,  
120 HydroBios<sup>®</sup>, 0.25 m<sup>2</sup> mouth opening) in seven discrete depth intervals (0-25, 25-65, 65-100, 100-  
121 135, 135-180, 180-230 and 230-280m). Zooplankton in the micro- and mesozooplankton size range  
122 were sampled by hauling vertically a 45 µm mesh Multinet from 280 m to the surface, while rare  
123 and larger sized zooplankton were sampled during an oblique haul with a 335 µm mesh Multinet  
124 lowered to 280 m and retrieved to the surface at a speed of 2 knots. For the 45 µm Multinet  
125 sampling, the water volume filtered per net ranged from 5 to 13 m<sup>3</sup>. Samples were preserved in 4%  
126 Borax buffered formalin, and after the cruise the zooplankton were identified, enumerated and  
127 measured for total length, and cephalothorax length for copepods.

128 Fish larvae and gelatinous macrozooplankton were sampled using a conical ring net (MIK, 3.5 m  
129 diameter opening, 25 m total length, 560  $\mu\text{m}$  body mesh size with 330  $\mu\text{m}$  mesh for the hindmost 1  
130 m and the cod end). The net was lowered to a given depth, measured by a mounted depth sensor  
131 (Scanmar<sup>®</sup>), using a fast wire pay-out, and towed at 2 knots for 40 min. Tow depth varied by  $\pm 3$  m  
132 during tows. Afterward, the net was retrieved at a high speed. Filtrating during the pay-out and  
133 retrieval phase was assumed to be ineffective at such high speed. The effective volume filtered was  
134 estimated from the tow path at depth apparent from the recorded profile of the depth sensor. Six  
135 discrete depths were sampled (45, 85, 120, 155, 205 and 255 m) during day (12:00-18:00 local  
136 time) and night (00:00-06:00 local time). Upon retrieval, the net was washed down and the cod-end  
137 content was transferred to 20 L transparent buckets (Cambro<sup>®</sup>). The buckets were kept on ice  
138 during processing, and the content was examined for fish larvae and gelatinous macrozooplankton  
139 (excluding siphonophores) within 45 min.

140 Gelatinous zooplankton were identified and measured alive using a dark field light table in  
141 transparent plexi-glass trays. After the screening, 10% of the MIK sample was preserved in 4%  
142 buffered formalin solution for later estimation of siphonophore abundance. Siphonophore  
143 abundance was difficult to estimate due to their colonial structure and tendency to disintegrate.  
144 However, the sampled siphonophore community consisted primarily of Calycothorans, hence we  
145 used only the anterior nectophore of the polygastric stage for species identification and enumeration  
146 (Bouillon *et al.*, 2004). Very few bracts of the sexual eudoxid stage were encountered.

147 Observed fish larvae were directly preserved in 96% ethanol, the leptocephali after being length  
148 measured in a stereomicroscope-video setup. The remainder of the sample was preserved in ethanol  
149 for later sorting, identification and measurement of fish larvae that were not observed during the  
150 initial screening. All length measurements were made to larval standard length. Fish larvae visually  
151 identified as *Anguilla* spp. were later verified as either *A. anguilla* or *A. rostrata* using molecular  
152 markers (Jacobsen *et al.*, 2016). Identification of other larval fish species was based on type  
153 specimens from an earlier study in the same area (Ayala *et al.*, 2016).

154 Information on the distribution and diel migration of acoustically reflecting organisms were  
155 obtained from a ship-mounted Simrad<sup>®</sup> EK60 38 kHz echosounder, which was run continuously  
156 during the vertical study. Signals were analyzed by Echoview<sup>®</sup> software, and data on volume  
157 backscatter at depth were interpolated using the Surfer<sup>®</sup> program.

158 *Data analyses:*

159 Distributional mean depths (MD) of plankton size intervals, genera or species were calculated as:

$$160 \quad MD = \sum_{k=0}^n D_k * W_k * C_k / \sum_{k=0}^n W_k * C_k$$

161 Where  $D_k$  is mean depth of stratum  $k$  (m),  $W_k$  is width of stratum  $k$  (m) and  $C_k$  is the estimated  
162 density of organisms in stratum  $k$  (no  $m^{-3}$ ).

163 For analysis of commonalities and differences in vertical distributions of plankton taxa we  
164 calculated a similarity matrix combining a double hierarchical classification and an ordered  
165 heatmap representation. The method considered Euclidean distances with a “complete link”  
166 classification. To compare both abundant and non-abundant taxa we used proportions in strata and  
167 solely strata in 45 m and below, since some taxa were not sampled in the uppermost stratum. In a  
168 schematic representation, the taxa were organized and grouped according to similarity in their  
169 relative abundances at depth.

170

## 171 **RESULTS**

### 172 *Hydrography*

173 The sampling site was positioned ca. 100 km north of the southern front of the STCZ. This front  
174 was characterized by declining isotherms at the southernmost part of the transect (Fig. 1 b). Water  
175 temperature was ca. 24-24.5°C in a mixed water layer extending to about 80 m depth. Below this  
176 layer a wide thermocline was apparent, with a decline in temperature to 19°C at 150 m (Fig. 2 a).  
177 Salinity was 36.6 in the mixing zone, and deeper, between 80 and 160 m depth, an intrusion of more  
178 saline water (~ 36.8) was apparent (Fig 1 c, Fig. 2 a). The intrusion at this sampling site had a  
179 double structure, a pattern also observed at other stations during the cruise. Further below the  
180 salinity declined, reaching 36.42 at 400 m and continuing the decline until at least the depth of 1000  
181 m (nearby CTD cast, data not shown).

182 Light levels measured at 14:30 UTM declined from 1000  $\mu\text{mol m}^{-2}\text{s}^{-1}$  at 10 m to 40  $\mu\text{mol m}^{-2}\text{s}^{-1}$  at  
183 100 m and 1.5  $\mu\text{mol m}^{-2}\text{s}^{-1}$  at 160 m (Fig. 2 b), and were below the detection limit at depths below  
184 250 m. The attenuation coefficient varied through the water column, showing peaks in the  
185 immediate surface layer and the in association with the deep chlorophyll *a* layer (Fig. 2 b).



186 Dissolved oxygen level was near 100% saturation in the upper 100 m but showed an abrupt drop to  
187 about 80 % across the upper thermocline, and stayed at this level further below (Fig. 2 b).  
188 Nitrate+nitrite levels were low in the upper 110 m ( $< 0.25 \mu\text{mol L}^{-1}$ ), increased to  $2 \mu\text{mol L}^{-1}$  at 130  
189 m and increased further at greater depths (Fig. 2 c). Silicate levels were in the order of  $1\text{-}2 \mu\text{mol L}^{-1}$ ,  
190 but were markedly lower between 60 and 130 m (Fig. 2 c).

#### 191 *Microplankton and snow particles*

192 The CTD fluorometer and extracted chlorophyll measurements showed similar vertical profiles of  
193 algal concentrations (Fig. 2 d). In the mixing zone at 0-80 m depth, the chlorophyll *a* concentration  
194 was low ( $\sim 0.08 \mu\text{g L}^{-1}$ ), but it increased further below and peaked in a deep chlorophyll maximum  
195 (DCM) of  $0.32 \mu\text{g L}^{-1}$  at about 120 m depth. Below the DCM the chlorophyll *a* concentration  
196 declined markedly to near zero at 200 m depth.

197 Particles detected by the Underwater Vision Profiler (UVP) were categorized into three groups  
198 based on their equivalent spherical diameter (Fig. 3 a). All three groups were found in high  
199 abundances near the surface, but they differed in their vertical distributions throughout the water  
200 column. Small particles showed a subsurface minimum of  $\sim 15$  particles  $\text{L}^{-1}$  in the depth range 20-60  
201 m, increasing to 25 particles  $\text{L}^{-1}$  at 160-200 m. In contrast, abundances of both medium and large  
202 particles steadily decreased with depth, reaching near zero particles below 250 m. Two  
203 characteristic components of the medium and large sized particles were identified as  
204 *Trichodesmium* colonies and radiolarians (Rhizaria) (Fig. 3 b). Both of these showed highest  
205 abundances above 60 m with another enhancement in abundance at 120-140 m (Rhizaria) or 140-  
206 200 m (*Trichodesmium*). Concentrations of ciliates and heterotrophic dinoflagellates based on bottle  
207 sampling showed both their highest levels above 150 m, but their peaks of abundance in the water  
208 column differed (Fig. 3 c). The dinoflagellates peaked close to the DCM, while abundances of  
209 ciliates were high in the mixed layer and showed a secondary peak below the DCM.

#### 210 *Mesozooplankton*

211 The vertical profile of total mesozooplankton from the  $45 \mu\text{m}$  Multinet sampling showed a  
212 characteristic peak at the surface, another at the 65-100 m depth interval, and very low abundances  
213 below 180 m (Fig. 4 a, Suppl. table 1). Diel changes in the combined vertical distribution of the  
214 community in the investigated upper 250 m were marginal, with a weak tendency of nighttime  
215 descent. There was, however, great variability in distribution patterns among the different

216 taxonomic groups (Suppl. fig. 1, Suppl. table 1). For example, *Oncaea* sp. showed no surface peak,  
217 (Fig. 4 g-h), while *Oithona* sp. copepods (Fig. 4 c) were distributed relatively deep with a peak  
218 around 150 m. Hydrozoans as *Amphicaryon acaule* and *Bougainvillia niobe* were distributed deep  
219 at day and shallower at night (Fig. 4 k-l). Additional differences were apparent within taxa for the  
220 naupliar and copepodite stages of copepods; e.g. *Clausocalanus* spp. nauplii tended to be deeper  
221 (Fig. 4 e-f) while *Oithona* sp. nauplii tended to be shallower (Fig. 4 c-d) compared to the respective  
222 copepodite stages.

223 The vertical distributions and migration patterns of mesozooplankton were related to size of  
224 organisms (Fig. 5 a). There was a general decline in MD, both for the copepods and for the group of  
225 other mesozooplankton. For the copepods the MD was about 70 m for length <500  $\mu\text{m}$ , and at these  
226 sizes (including the nauplii stages) the distances of diel vertical migration (DVM) were minor  
227 (<10m). In the copepod length range of 500-1000  $\mu\text{m}$  the MD declined from the 70 to 90 m depth,  
228 with a DVM of 20-30 m (ascent at night). The largest size group for which the MD could be  
229 calculated (1300  $\mu\text{m}$ ) was found at depth 110-140 m and showed a nighttime descent; this group was  
230 dominated by *Haploptilus* spp, which had an uncommon DVM behavior (Fig 5 b-c). In the group of  
231 non-copepod zooplankton, there was a more pronounced influence from size, and MD changed  
232 from 20-60 m to 90-130 m across the length range 100-900  $\mu\text{m}$ , while the DVM was 10-50 m,  
233 primarily with an ascent at night.

234 Underlying the apparent size-dependence of MD and DVM for copepods, there was a significant  
235 variability in MD and DVM related to stage and taxon. There was a span in MD from 40-50 m for  
236 copepodite stages of *Acartia* sp. and *Clausocalanus* sp., to 180-200 m for *Marmonilla* sp. and  
237 *Pleuromamma* sp. (Fig. 5 b). Between these extremes, the MD's of the other taxa were spread quite  
238 evenly. The general range of DVM was 10-20 m, but examples of a wider range of migration were  
239 also seen (Fig. 5 b-c). Our findings also showed that adults of different species of the same genera  
240 can behave quite differently, e.g. *Clausocalanus paulus* vs. *C. furcatus*. and *Oncaea media* vs. *O.*  
241 *mediterranea* (Fig. 5 c). This appears, however, not to be in accordance with the general tendency  
242 of larger size being at greater depth, given that *Clausocalanus paulus* is smaller than *C. furcatus*  
243 (~560  $\mu\text{m}$  vs. ~800 $\mu\text{m}$ ) and *Oncaea media* is smaller than. *O. mediterranea* (~370  $\mu\text{m}$  vs. ~660  
244  $\mu\text{m}$ ).

245 *Macroplankton*

246 Most of the macroplankton caught by the large ring net were distributed relatively deep at day  
247 between 80 and 180 m, and shallower at night above 120 m (Suppl. table 1). For some taxa within  
248 this group, the abundances integrated for the sampled water column were higher during night than  
249 during day. Net avoidance at day is unlikely the explanation because these macroplankton cannot  
250 visually detect the approaching net; rather, a part of the population may be distributed deeper than  
251 our sampling depth at daytime. *Bougainvillea niobe* was among the most numerically abundant; this  
252 species migrated from about 130 m at day to 90 m at night (Fig. 4 m). The siphonophore  
253 *Amphicaryon acaule* showed a strong upward shift in MD from about 160 m to 70 m between day  
254 and night (Fig. 4 n). Other siphonophores stayed deeper during nighttime, and their MD changed  
255 from about 150 m at day to 110 m at night (Fig. 4 o).

#### 256 *Leptocephali larvae*

257 We collected 164 *A. anguilla* and 19 *A. rostrata* larvae during the two series of ring net hauls. The  
258 vertical distribution of *A. anguilla* showed a pronounced diel difference: larval abundance peaked at  
259 155 m in daytime (82% of larvae were sampled in the two depth strata 120 m and 155 m), but at  
260 nighttime larval abundance peaked at 45 m (53% of larvae present at the stratum 45 m; Fig 6 a), and  
261 was also more dispersed in the water column. The MD at day was close to the observed depth of  
262 peak concentration (160 m vs 155 m), while at night the MD was somewhat deeper (110 m vs 45 m)  
263 (Fig. 8 a). Although the diel patterns of vertical distribution of *A. rostrata* were less apparent due to  
264 the relatively low catch of this species, findings also indicate peaks in densities at 155 m at day and  
265 at 45 m at night (Fig. 6 b), while the MD's are slightly shallower than for *A. anguilla* (150 m at day  
266 and 90 m at day, Fig 8 a). Mean body lengths for *A. anguilla* were 14.1 and 14.5 mm in daytime  
267 and nighttime samples, respectively, and for *A. rostrata* 14.4 and 17.5 mm, respectively. Larval  
268 mean lengths tended to increase with depth at day, whereas no such tendency was seen at night  
269 (Fig. 6 d-f).

270 Other species of leptocephali larvae were generally larger than the anguillid leptocephali, and due to  
271 visual net avoidance they were poorly represented in the daytime samples. Only the nighttime  
272 vertical distribution of the combined group of leptocephali larvae is presented here, illustrating the  
273 same pattern as for the anguillid larvae: increasing density towards the shallowest stratum of  
274 sampling (Fig. 6 c).

#### 275 *Other fish larvae*

276 We identified 16 taxonomic groups of fish larvae other than the leptocephali; these were identified  
277 to the species or family level (Suppl. table 1). The diel vertical distribution differed markedly  
278 between several of these groups (Fig. 7): Some had their peak distribution at day in the mid-layer  
279 (depths 120-155 m) but the concentration could locally be high with almost all larvae found at the  
280 same depth (e.g. *Hygphum taaningi*, Fig. 7 e), or the larvae could be more dispersed in the lower  
281 water column (e.g. *Scopelarchus* sp., Fig. 7 b). At night, the overall majority of individuals of each  
282 taxon was found at the shallowest depth (e.g. *Evermannellidae* spp., Fig. 7 a), in the mid-layer (e.g.  
283 *Sternoptychidae diaphana*, Fig. 7 f) or at the deepest depth investigated (*Scopelarchus* sp., Fig. 7 b).  
284 The large variation in distribution patterns of larvae was reflected in their MD's (Fig. 8 b): two  
285 species were either outstandingly shallow (*Ceratoscopelus warmingii*) or deep (*Scopelarchus* sp.),  
286 whereas the mean depths of the others were distributed quite evenly between 70 m and 170 m. Both  
287 downward and upward migrations between day and night were observed, the vertical migration  
288 range was for most species in the order of 20-30 m, but a few species migrated 40-50 m (Fig. 8 b).

289

#### 290 *Fish and other organisms from acoustics*

291 The vertical distribution of organisms reflecting 38 kHz signals was described for a 48-h period,  
292 from 1:00 on the 31 March to 23:00 on the 1st April (Fig. 9). At night, acoustic reflections showed  
293 an elevated abundance of organisms in the upper 140 m. Separate layers of enhanced reflection  
294 were apparent. Just before daybreak (> 10 PAR at 10:00 UTM), a group of organisms descended  
295 relatively quickly, reaching ~300 m at 10:30 and ~500 m at 12:00. In contrast, other organisms from  
296 the series of bands within the upper 250 m showed a more gradual and shorter descent (max. ~50 m  
297 descent of separate band), reaching their deepest level at noon when light intensity was at its  
298 highest. These migration patterns were reversed after 12:00 UTM, and were repeated in the  
299 following 24 h period (Fig. 9).

#### 300 *Plankton community patterns*

301 A cluster analysis on vertical distribution of all abundant mesozooplankton and ichthyoplankton  
302 taxa illustrated the diversity of distribution patterns, but also revealed a separation of taxa into  
303 distribution types (Suppl. fig. 1). At a “semi R-square” level above 50% we separated 6 clusters of  
304 distinct characteristics in the daytime sampling (Suppl. fig. 1 a). Three of these showed a  
305 characteristic concentration within a single stratum, one of these types, with a concentration in the

306 85 m stratum, was dominated by mesozooplankton taxa, while fish larvae dominated in two other  
307 types (concentration at 45m or 120 m). A large group of taxa was characterized by their bimodal  
308 vertical distribution showing peak abundances in the 85 m and 155 m strata; this was the general  
309 vertical distribution pattern for most of the mesozooplankton. Another group, in which we find the  
310 two anguillid eels, constituted a fifth type showing enhanced abundance in the 120 m and 155 m  
311 strata. The sixth group was found relatively deep (in 155 m stratum or below); however, only few  
312 taxa exhibited this distribution pattern. The analysis inferred further clusters within these main  
313 clusters, and the general picture of the analysis was a high diversity in patterns of plankton  
314 distribution.

315

## 316 **Discussion**

317 Our study was focused on plankton distribution in the upper 250 m of the 5000 m deep water  
318 column with the expectation that the majority of the community, including the eel larvae, would be  
319 distributed here. This interval covers the euphotic zone of sufficient light for primary production  
320 and for visual feeding by the fish larvae (about  $0.02 \mu\text{mol m}^{-2} \text{s}^{-1}$ ; Blaxter, 1980). Further, our  
321 observations of a marked decline in abundances of most of the investigated taxa in the deepest  
322 sampled stratum (midpoint 255 m) suggests that, by sampling to this depth, we included most of the  
323 relevant plankton biomass. The indication in our data that most planktonic organisms in the area  
324 had this relatively shallow distribution is supported by findings during studies in other oligotrophic  
325 areas which sampled to larger depths (>1000 m). In those studies, modal depths of most  
326 investigated plankton species were also found in the interval of 25-150 m (e.g. Longhurst, 1985;  
327 Sameoto, 1986). A smaller proportion of the plankton, however, primarily inhabit the deeper  
328 layers; e.g. Deevey and Brooks (1977) found in a study off Bermuda that abundances of plankton  
329 species residing below 500 m (in the 500-1000 m layer) could be up to 20% of the abundances  
330 above 500 m.

331 The high diversity in plankton distributions in the investigated water layer reflected the large  
332 variability in physical conditions. Within the first 250 m of the water column there was a significant  
333 change in light, temperature and water density, and within the pycnocline (80-150 m) we found a  
334 strong peak in chlorophyll *a* and a marked intrusion of relatively high-saline water. Thus a wide  
335 range of habitual niches are available to the mesozooplankton and ichthyoplankton, and

336 characteristic peaks of distribution within certain depth strata were seen for many organisms.  
337 Consequently, the clustering of organisms based on distributional similarities showed that in  
338 addition to bulk-water characteristics, there were also significant fine-scale variabilities that  
339 influenced the distributional patterns for both mesozooplankton and ichthyoplankton.

340 A large number of the investigated taxa showed systematic polymodality in their vertical  
341 distribution. The layer immediately below the uppermost surface (measured at 45 m depth)  
342 appeared unsuitable for most taxa, leading to low abundances here. While the mesozooplankton  
343 organisms often were abundant above (12 m stratum) and below (85 m stratum); this led to two  
344 modes in the vertical distribution. For many organisms there was a tendency of another low in  
345 abundance at the central pycnocline at about 120 m, within the salinity intrusion and the chlorophyll  
346 *a* maximum. This tendency of several modes in distribution was seen for much of the  
347 mesozooplankton, both during daytime and nighttime sampling, for much of the mesozooplankton,  
348 while for the ichthyoplankton the pattern of distribution was unimodal for most taxa.

349 The concentration at specific depth was evident for the two anguillid eel larvae. At daytime, the  
350 larvae congregated in the 155 m stratum at a concentration about seven times as high as the average  
351 of the other abundance estimates in the water column, and at nighttime the concentration in the 45  
352 m stratum was three times as high as the average of other estimates. Thus, at the investigated site,  
353 most of the anguillid leptocephali were below 100 m at daytime while the majority migrated to  
354 above 100 m depth at night. Interestingly, peaks in eel larvae distribution coincided with peaks in  
355 abundances of sampled hydrozoans, as apparent when comparing Fig 6 a-b with Fig. 5 k-l. The  
356 hydrozoans have been proposed as possible food items for the leptocephali larvae (Riemann et al.  
357 2010), and a study from the same cruise found eel larval gut contents dominated by gene sequences  
358 of taxa belonging to Hydrozoa (Ayala et al., in press).

359 The observations of a deeper distribution of anguillid eel larvae during daytime, and a shallower  
360 distribution during nighttime are in accordance with other findings for the species during the  
361 winter/spring period. Castonguay and McCleave (1987) found significant abundance peaks in  
362 specific depth strata as well: In their study, the maximal concentration at depth was seen at night  
363 and was here about nine times the average of the other depth strata. Accordingly, the day and night  
364 peak concentrations of larvae occurred within the wide pycnocline, and the tendency of an increase  
365 in larval mean length with increasing sampling depth during daytime are also apparent in the data  
366 presented by Schoth and Tesch (1984).

367 The observed diel migration (~70m) of *Anguilla* sp. was of exceptional magnitude compared to  
368 migrations of most other fish larvae in our study, which ranged only 10-30 m. Migration distances  
369 of oceanic fish larvae are commonly in the lower range; for example, in a study of the fish larval  
370 community off the Canary Islands, Rodriguez *et al.* (2006) observed relatively short migration  
371 distances of 5-20 m for most species, and similar to our study, they observed both upward and  
372 downward migrations during night. The different species of fish larvae we observed apparently  
373 utilized different parts of the water column; some were concentrated in relatively deep water, some  
374 in the shallow layer, and others were more dispersed in the mid-layer. Thus, while the vertical  
375 distributions of fish larvae overlapped to different degrees, the calculated midpoints of distributions  
376 extended throughout much of the water column.

377 We used acoustic measurements and the diel movement of bands of enhanced backscatter to  
378 describe migratory patterns of plankton and fish at a finer temporal scale than our day-night  
379 sampling. Stratification of the backscatter is a common observation in acoustic surveys, and the  
380 different bands of enhanced backscatter have been related to different taxonomic composition of  
381 organisms (e.g. Lawson *et al.*, 2004). While we cannot directly link certain bands to specific taxa,  
382 the patterns of backscatter in the uppermost water column during night are in accordance with the  
383 observations of peaking distributions of organisms in the pycnocline and around the high-saline  
384 intrusion at 80-130 m depth (Fig 9).

385 The acoustic observations complement our day-night sampling by showing the diel migration as a  
386 gradual descent to, and ascent from, the deepest positions of given organisms. The descent was  
387 initiated at the first light at the surface, and the return was finished at time of complete darkness.  
388 Successively, the vertical positions of organisms were stable during night, with a slight tendency of  
389 deeper distribution at midnight, until a new descent in the morning. From the acoustic  
390 measurements the general migration distances in the upper part of the water column were  
391 interpreted to be about 50 m, which is in the upper range compared to migration distances of most  
392 of the (smaller) organisms that were included in our day-night sampling campaign. The descent of  
393 the upper set of distribution bands reached to about 270 m, which is within the range of the general  
394 light threshold for larval fish feeding (Fig. 9). In the echogram some bands of acoustic backscatter  
395 apparent at night descended much deeper than the 50 m; these are likely related to movement of  
396 mesopelagic fish which are commonly observed to descend to more than 500 m depth (e.g. Badcock  
397 and Merrett, 1976; D'Elia *et al.*, 2016).

398 In conclusion the study illustrates the great physical and biological variabilities of the area of eel  
399 larvae distribution at STCZ, and points out a range of commonalities and differences between  
400 plankton taxa at the mesozooplankton and ichthyoplankton levels. Irrespective of the oligotrophic  
401 nature of this oceanic area, the diversity of the plankton community – in terms of taxonomy and  
402 distribution patterns - was notably high. Plankton organisms were highly concentrated in specific  
403 strata, and several peaks in their vertical distribution could often be seen. These presumably are  
404 linked to the variable hydrography around the pycnocline. The anguillid eels concentrate in the  
405 lower part of the pycnocline at daytime, and their prevalence in a water layer with enhanced  
406 abundances of hydrozoans indicates these organisms as potential prey item for the eel larvae. For  
407 further understanding and modelling of the early life characteristics of eel across their extensive  
408 area of distribution, it is necessary to incorporate the prominent small-scale variability and diversity  
409 of their immediate physical and biological environments.

410

411

412

### 413 **Acknowledgements**

414 This study was supported by the Carlsberg Foundation, Denmark (2012\_01\_0272); Danish Centre  
415 for Marine Research (2013\_02) and the Danish Council for Independent Research/Marie Curie  
416 (Mobilex: DFF-1325-00102B to CJ). The authors have no conflicts of interest related to the  
417 presented work. We thank colleagues and the crew of the Danish research vessel, DANA, for their  
418 helpful assistance during field sampling and sample processing.

419



420 **References**

- 421 Andersen, N. G., Nielsen, T. G., Jakobsen, H. H., Munk, P., & Riemann, L. (2011). Distribution  
422 and production of plankton communities in the subtropical convergence zone of the Sargasso Sea.  
423 II. Protozooplankton and copepods. *Marine Ecology Progress Series*, 426, 71-86.
- 424 Ayala, D., Riemann, L., & Munk, P. (2016). Species composition and diversity of fish larvae in the  
425 Subtropical Convergence Zone of the Sargasso Sea from morphology and DNA barcoding.  
426 *Fisheries oceanography*, 25(1), 85-104.
- 427 Ayala, D.J., Munk, P., Lundgreen, R.B.C., Traving, S.J., Jaspers, C., Jørgensen, T.S., Hansen, L.H.  
428 & Riemann, L. (in press). Gelatinous plankton is central to the diet of European eel (*Anguilla*  
429 *anguilla*) larvae in the Sargasso Sea. *Scientific Reports*
- 430 Badcock, J., & Merrett, N. R. (1976). Midwater fishes in the eastern North Atlantic—I. Vertical  
431 distribution and associated biology in 30 N, 23 W, with developmental notes on certain myctophids.  
432 *Progress in Oceanography*, 7(1), 3-58.
- 433 Blaxter, J. H. S. (1980). Vision and feeding of fishes. In: *Fish Behaviour and its Use in the Capture*  
434 *and Culture of Fishes* (Vol. 5, pp. 32-56). International Center for Living Aquatic Resources  
435 Management Manila, Philippines.
- 436 Bouillon, J., Medel, M. D., Pages, F., Gili, J. M., Boero, F. and Gravili, C. (2004) Fauna of the  
437 Mediterranean Hydrozoa. *Scientia Marina*, 68, 5-449.
- 438 Castonguay, M., & McCleave, J. D. (1987). Vertical distributions, diel and ontogenetic vertical  
439 migrations and net avoidance of leptocephali of *Anguilla* and other common species in the Sargasso  
440 Sea. *Journal of Plankton Research*, 9(1), 195-214.
- 441 Cushman-Roisin, B. (1984). On the maintenance of the Subtropical Front and its associated  
442 countercurrent. *Journal of physical oceanography*, 14(7), 1179-1190.
- 443 Deevey, G. B., & Brooks, A. L. (1977). Copepods of the Sargasso Sea off Bermuda: species  
444 composition, and vertical and seasonal distribution between the surface and 2000 m. *Bulletin of*  
445 *Marine Science*, 27(2), 256-291.

446 D'Elia M, Joseph D. Warren, Ivan Rodriguez-Pinto, Tracey T. Sutton, April Cook, Kevin M.  
447 Boswell, Diel variation in the vertical distribution of deep-water scattering layers in the Gulf of  
448 Mexico, Deep Sea Research Part I: Oceanographic Research Papers, Volume 115, 2016, Pages 91-  
449 102, <http://dx.doi.org/10.1016/j.dsr.2016.05.014>.

450 Eriksen, C. C., Weller, R. A., Rudnick, D. L., Pollard, R. T., & Regier, L. A. (1991). Ocean frontal  
451 variability in the frontal air-sea interaction experiment. *Journal of Geophysical Research: Oceans*,  
452 96(C5), 8569-8591.

453 Gasol JM, del Giorgio PA, Duarte CM (1997) Biomass distribution in marine planktonic  
454 communities. *Limnol Oceanogr* 42:1353–1363

455 Halliwell Jr, G. R., Ro, Y. J., & Cornillon, P. (1991). Westward-propagating SST anomalies and  
456 baroclinic eddies in the Sargasso Sea. *Journal of physical oceanography*, 21(11), 1664-1680.

457 Jacobsen, M. W., Smedegaard, L., Sørensen, S. R., Pujolar, J. M., Munk, P., Jónsson, B.,  
458 Magnussen, E. & Hansen, M. M. (2017). Assessing pre-and post-zygotic barriers between North  
459 Atlantic eels (*Anguilla anguilla* and *A. rostrata*). *Heredity*, 118(3), 266.

460 Lawson GL, Peter H. Wiebe, Carin J. Ashjian, Scott M. Gallagher, Cabell S. Davis, Joseph D.  
461 Warren, Acoustically-inferred zooplankton distribution in relation to hydrography west of the  
462 Antarctic Peninsula, Deep Sea Research Part II: Topical Studies in Oceanography, Volume 51,  
463 Issue 17, 2004, Pages 2041-2072,

464 Longhurst, A. R. (1985). The structure and evolution of plankton communities. *Progress in*  
465 *Oceanography*, 15(1), 1-35.

466 Miller, M. J. (2015). Nighttime vertical distribution and regional species composition of eel larvae  
467 in the western Sargasso Sea. *Regional Studies in Marine Science*, 1, 34-46.

468 Miller, M. J., Bonhommeau, S., Munk, P., Castonguay, M., Hanel, R., & McCleave, J. D. (2014). A  
469 century of research on the larval distributions of the Atlantic eels: a re-examination of the data.  
470 *Biological Reviews*, 90(4), 1035-1064.

471 Munk, P., Hansen, M. M., Maes, G. E., Nielsen, T. G., Castonguay, M., Riemann, L., ... & Bachler,  
472 M. (2010). Oceanic fronts in the Sargasso Sea control the early life and drift of Atlantic eels.  
473 *Proceedings of the Royal Society of London B: Biological Sciences*, rspb20100900.

474 Richardson, K., & Bendtsen, J. (2017). Photosynthetic oxygen production in a warmer ocean: the  
475 Sargasso Sea as a case study. *Phil. Trans. R. Soc. A*, 375(2102), 20160329.

476 Riemann, L., Nielsen, T. G., Kragh, T., Richardson, K., Parner, H., Jakobsen, H. H., & Munk, P.  
477 (2011). Distribution and production of plankton communities in the subtropical convergence zone  
478 of the Sargasso Sea. I. Phytoplankton and bacterioplankton. *Marine Ecology Progress Series*, 426,  
479 57-70.

480 Rodríguez, J. M., Hernández-León, S., & Barton, E. D. (2006). Vertical distribution of fish larvae in  
481 the Canaries-African coastal transition zone in summer. *Marine Biology*, 149(4), 885-897.

482 Sameoto, D. D. (1986). Influence of the biological and physical environment on the vertical  
483 distribution of mesozooplankton and micronekton in the eastern tropical Pacific. *Marine Biology*,  
484 93(2), 263-279.

485 Schmidt J (1923) The Breeding Places of the Eel. *Philosophical Transactions of the Royal Society*  
486 of London. Series B 211: 179-208

487 Schoth, M., & Tesch, F. W. (1982). Spatial distribution of 0-group eel larvae (*Anguilla* sp.) in the  
488 Sargasso Sea. *Helgoländer Meeresuntersuchungen*, 35(3), 309.

489 Steinberg, D. K., Carlson, C. A., Bates, N. R., Johnson, R. J., Michaels, A. F., & Knap, A. H.  
490 (2001). Overview of the US JGOFS Bermuda Atlantic Time-series Study (BATS): a decade-scale  
491 look at ocean biology and biogeochemistry. *Deep Sea Research Part II: Topical Studies in*  
492 *Oceanography*, 48(8), 1405-1447.

493 Ullman, D. S., Cornillon, P. C., & Shan, Z. (2007). On the characteristics of subtropical fronts in  
494 the North Atlantic. *Journal of Geophysical Research: Oceans*, 112(C1).

495 Williams RG (2001) Ocean subduction. In: Steele JH, Turekian KK, Thorpe SA (eds) *Encyclopedia*  
496 *of ocean sciences*. Academic Press, pp 1982–1992

497

498 **Legends to figures**

499

500 **Figure 1**

501 Area of sampling. a) Transect at 62°45'W (line) and sampling position (dot) in the southern  
502 Sargasso Sea for this study; contour lines indicate SST from satellite observations. Hydrographical  
503 sections along the transect for b) temperature (°C) and c) salinity; vertical lines indicate sampling  
504 position for the vertical study

505 **Figure 2**

506 Depth profiles at the vertical study site: a) Temperature, salinity and water density; b) oxygen, light  
507 radiance and light attenuation coefficient; c) NO<sub>3</sub>+NO<sub>2</sub> and silicate; and d) fluorescence and  
508 chlorophyll *a*. Measurements in a) and b) and fluorescence are from CTD cast; measurements in c)  
509 and chlorophyll *a* are from water bottle sampling.

510 **Figure 3**

511 Abundances of a) Marine snow (0.05-0.53, 0.53-1.06, 1.06-4.0 mm); b) *Trichodesmium* and  
512 Rhizaria; and c) ciliates and heterotrophic dinoflagellates. Measurements in a) and b) are from  
513 profiling by video recorder; measurements in c) are from water bottle sampling.

514 **Figure 4**

515 Day (open symbol) and night (closed symbol) vertical distributions of selected plankton taxa and  
516 stages. a) to j) Mesozooplankton profiles based on 45 µm vertical Multinet hauls in strata, average  
517 abundances in stratum (no. m<sup>-3</sup>). k) and l) Macrozooplankton profiles based on horizontal 550 µm  
518 MIK net hauls at depth (no. 1000 m<sup>-3</sup>).

519 **Figure 5**

520 Day-night changes in depth (m) of the abundant copepod taxa. a) Average length (within intervals  
521 of 100µm) at depth (m) for all copepods. b) Average depth at day versus night for a number of  
522 genera in copepodite stages. c) Average depth at day versus night of adult copepods identified to  
523 species.

524 **Figure 6**

525 Vertical distribution and mean sizes of leptocephali species. Day (open symbol) and night (closed  
526 symbol) distributions of a) *Anguilla anguilla* and b) *A. rostrata* (no 1000 m<sup>-3</sup>). c) Night distribution  
527 of non-anguillid leptocephali larvae (no 1000 m<sup>-3</sup>). d) Mean lengths at depth during day and night  
528 for d) *A. anguilla* and f) *A. rostrata* (mm). Based on MIK hauls at nominal depths (symbol ±3m).

529 **Figure 7**

530 Vertical distribution of selected fish larvae species based on MIK hauls at nominal depths (symbol  
531 ±3m); values in no. 1000 m<sup>-3</sup>.

532 **Figure 8**

533 Average depth (m) at day versus night for common fish larvae species in the area. The two anguillid  
534 species are highlighted by bold text and dashed lines.

535 **Figure 9**

536 Lower graph: Acoustic backscatter by ship-mounted 38KHz echo sounder, in dB, as given by bar to  
537 the right. From 01:00 (UTM) on the 31 March to 23:00 on the 1st April. White line off left axis  
538 illustrates the salinity profile; lines undulating to depth illustrate calculated depths of given light  
539 intensities; white upper line: 1.5 μmol m<sup>-2</sup> s<sup>-1</sup>, grey lower line: 0.02 μmol m<sup>-2</sup> s<sup>-1</sup>. Upper graph:  
540 surface light intensity during the same period, from ship-mounted PAR sensor.

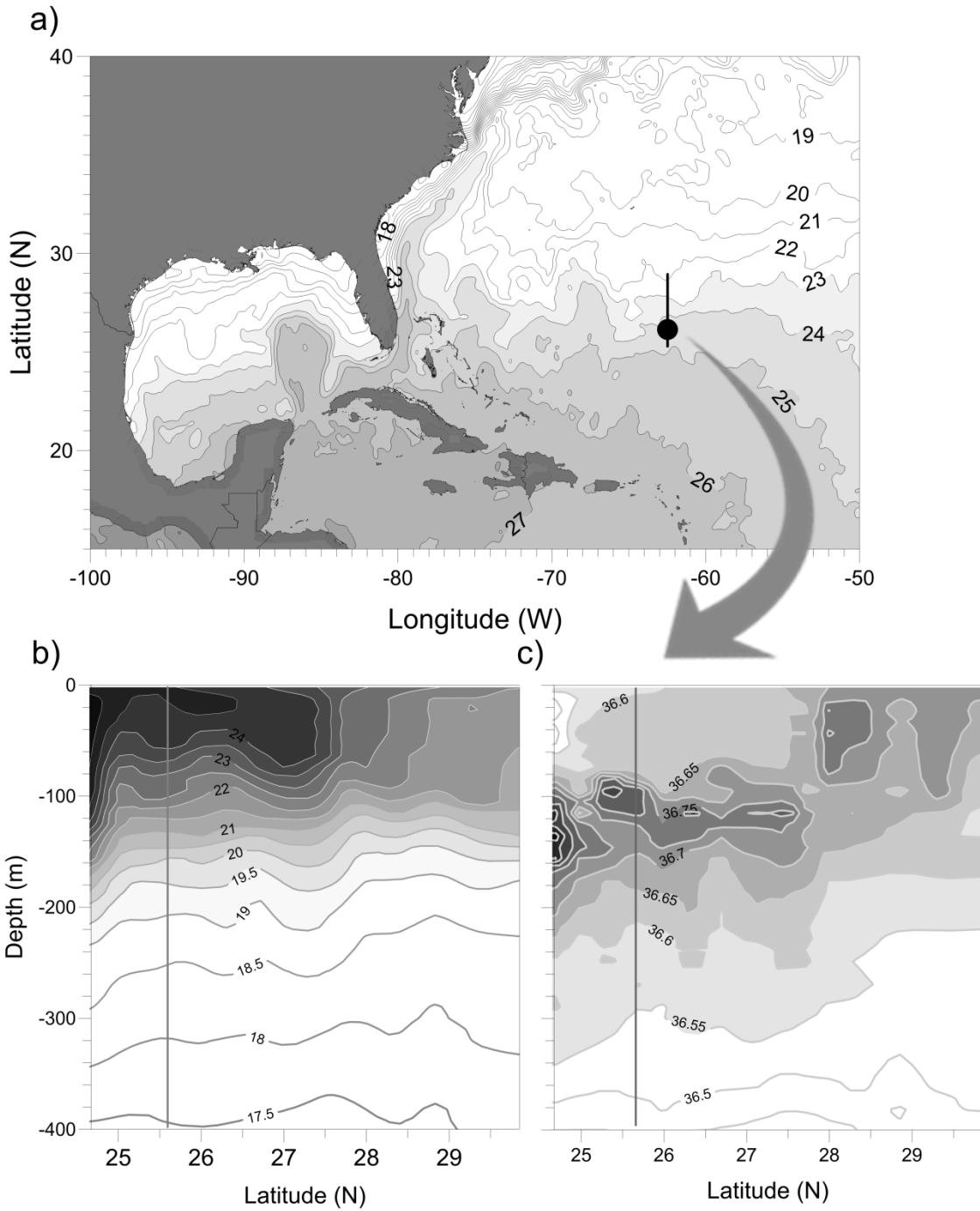
541

542 **Supplementary figure 1.**

543 Cluster diagrams of relatively abundant plankton taxa (abundance above 10% within three groups:  
544 copepods, non-copepod mesozoplankton, and ichthyoplankton). Coloring of presence within the 6  
545 strata is represented by a colorbar to the right; presence of each taxon accumulate to 100%. a)  
546 Cluster diagram for daytime sampling. Six clusters, separated by >50% level, are marked by red  
547 rectangles. Fish larvae taxon is indicated by asterisk. b) Cluster diagram for nighttime sampling.

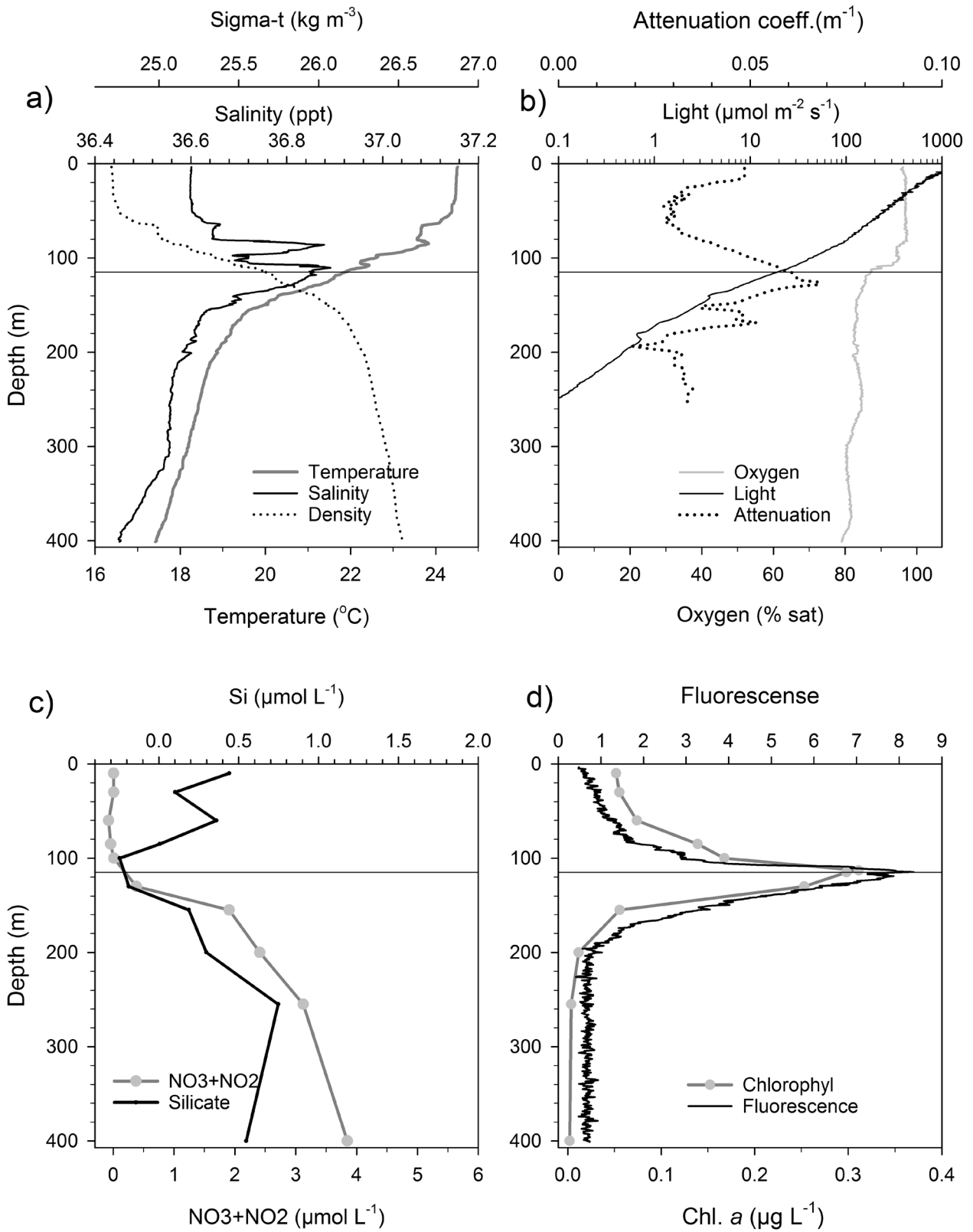
548 **Supplementary Table 1**

549 Abundances of mesozooplankton (no  $m^{-3}$ ), macroplankton (no 1000  $m^{-3}$ ) and fish larvae (no 1000  
550  $m^{-3}$ ) from vertically stratified sampling at average depths 12, 45, 85, 120, 155, 205 and 255 m  
551 during day and night periods. The 12 m depth stratum only presented for mesozooplankton.



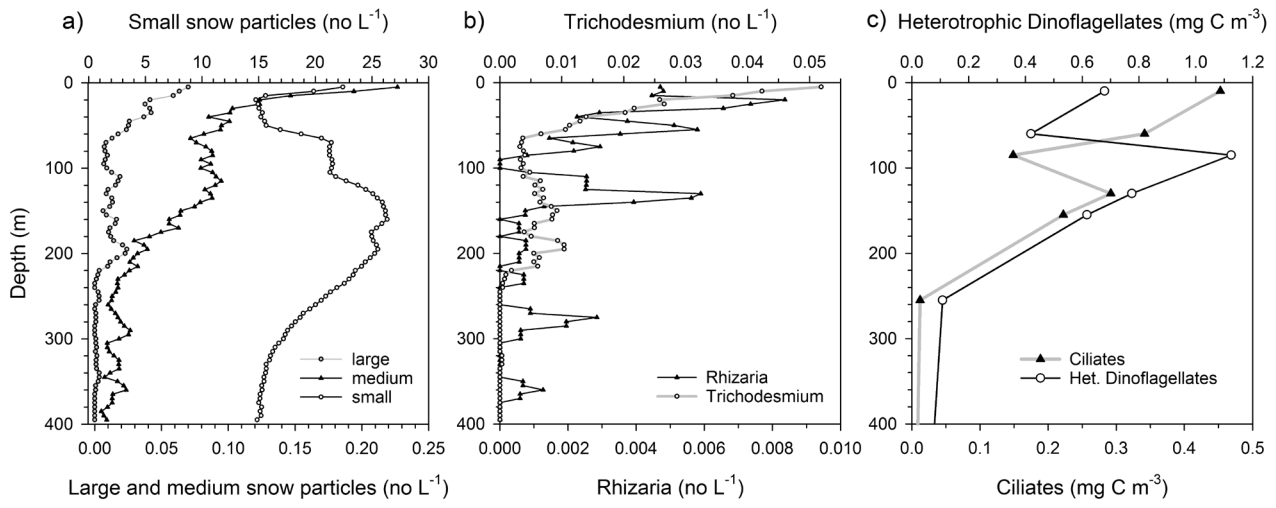
552

553 Figure 1



554

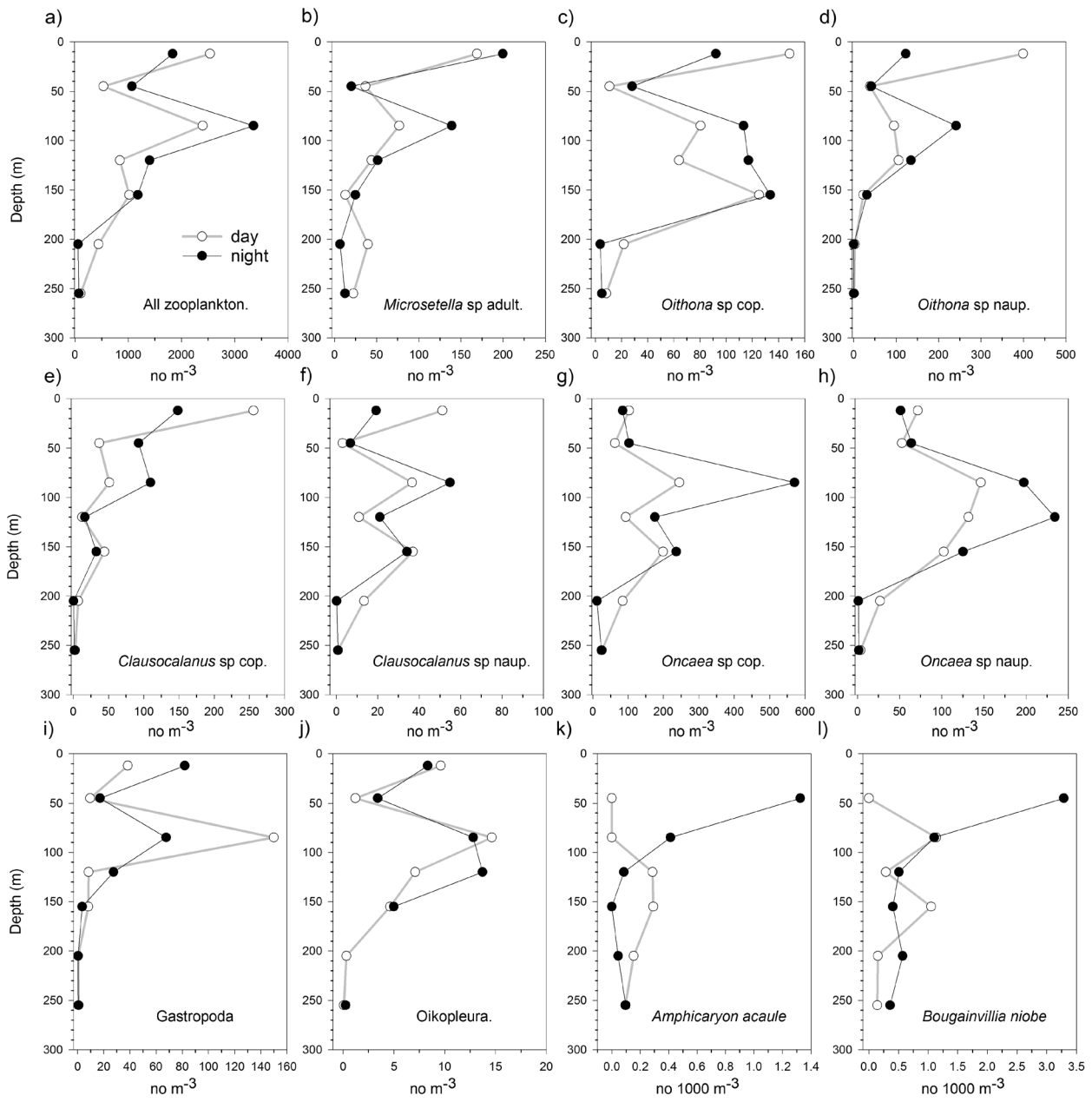
555 Figure 2



556

557 Figure 3

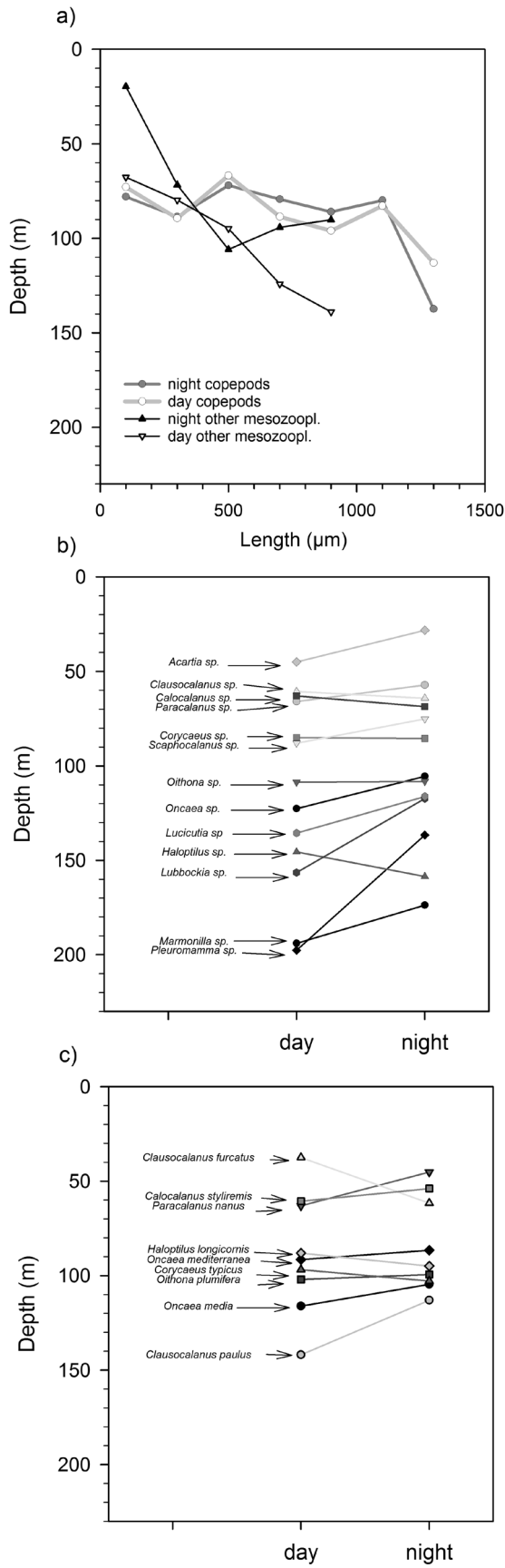




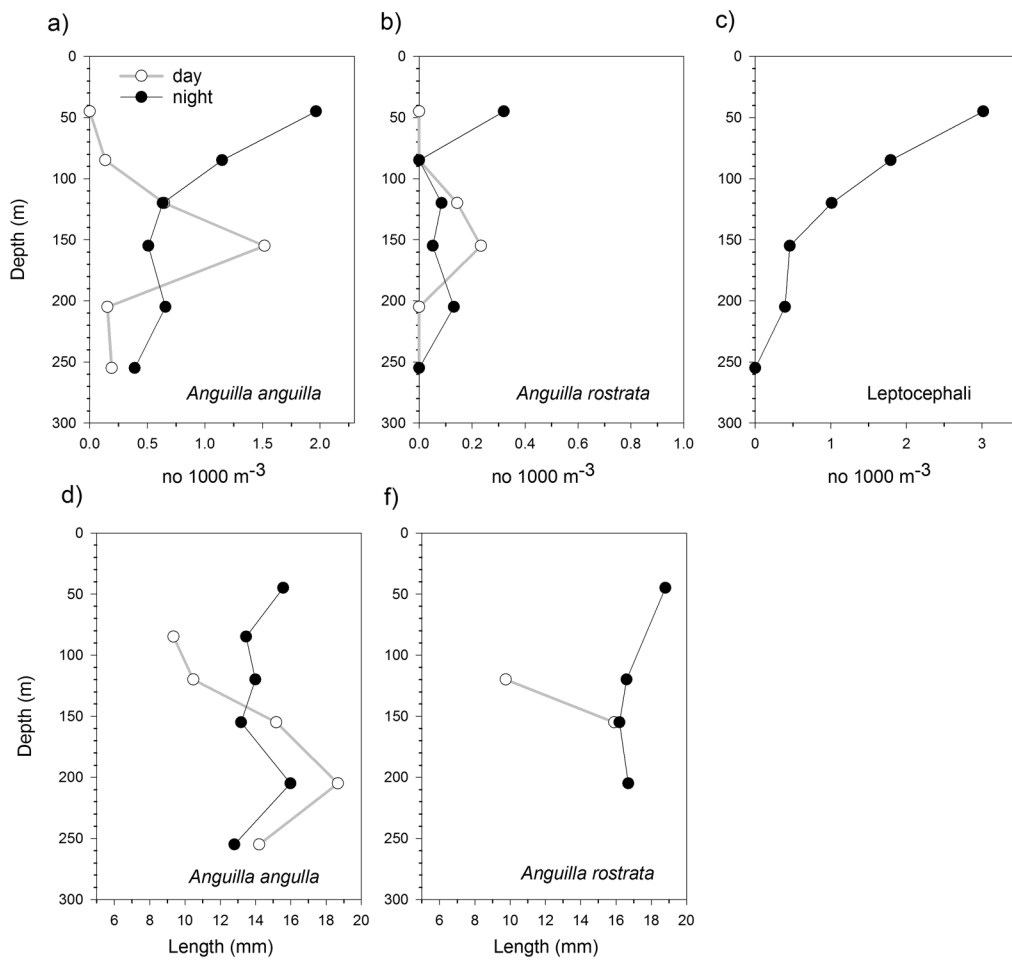
558

559 Figure 4

560

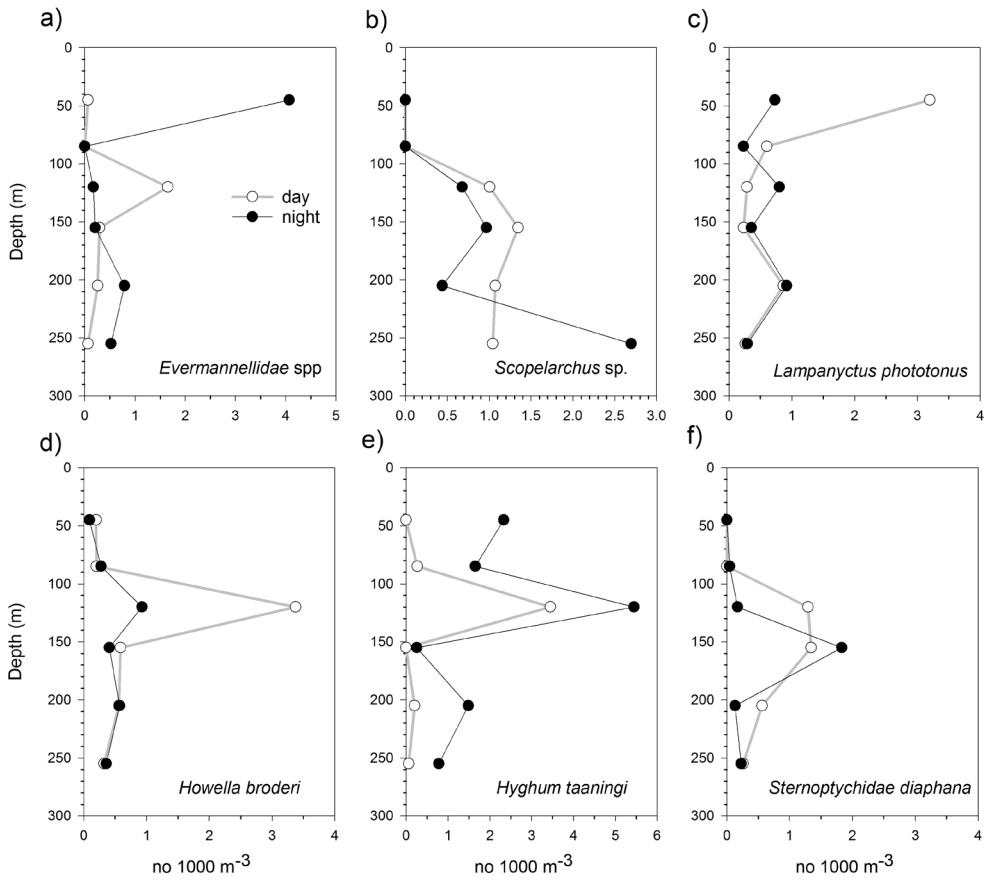


561 Figure 5



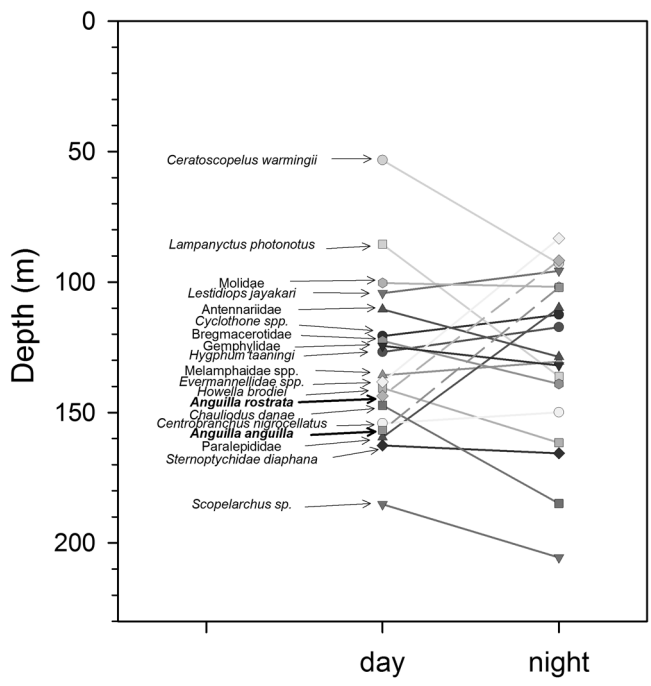
562

563 Figure 6



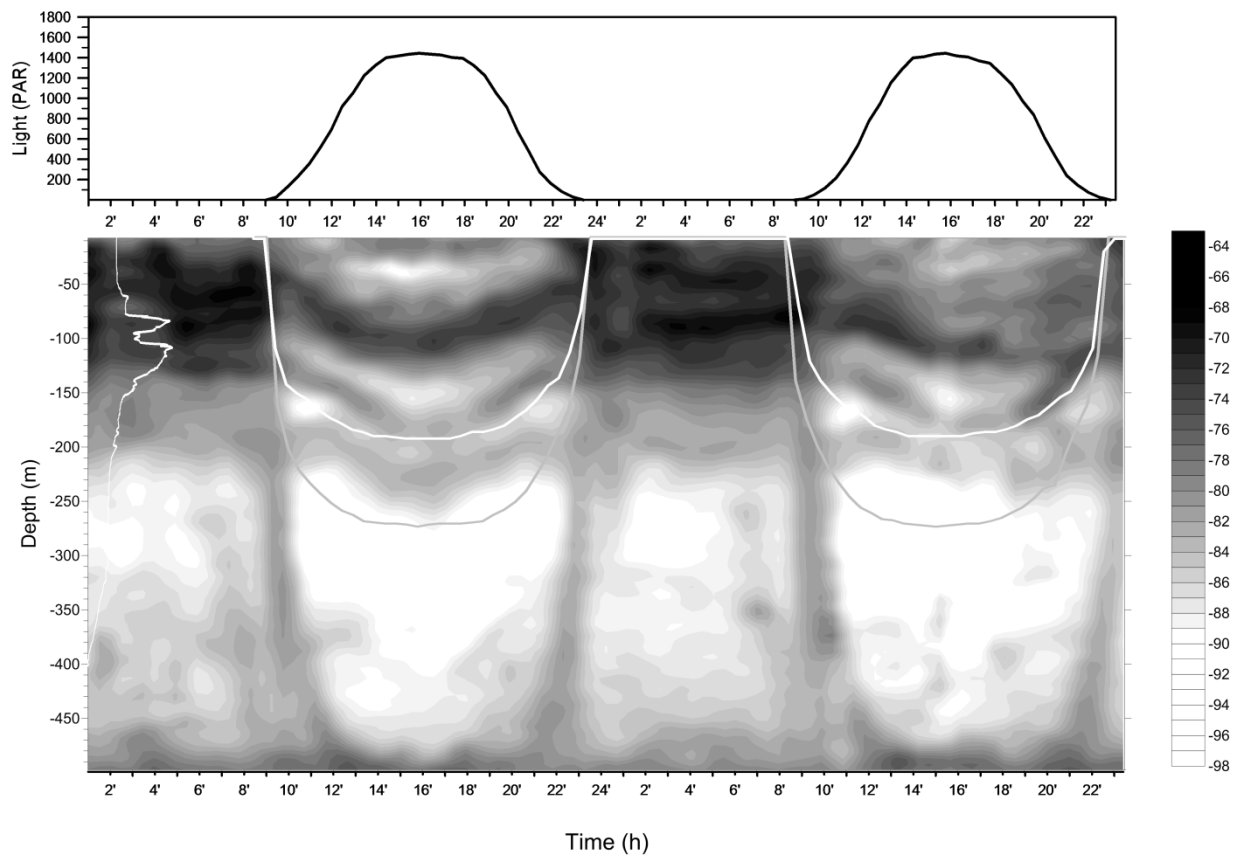
564

565 Figure 7



566

567 Figure 8



568

569 Figure 9

570